

Supplemental Data

The *In Vivo* Pattern of Binding of RAG1 and RAG2 to Antigen Receptor Loci

Yanhong Ji, Wolfgang Resch, Elizabeth Corbett, Arito Yamane, Rafael Casellas, and David G. Schatz

Inventory of Supplemental Information:

Figure S1, related to Figures 1-4

Figure S2, related to Figure 1

Figure S3, related to Figures 1-4

Figure S4, related to Figure 1

Figure S5, related to Figures 2 and 4

Figure S6, related to Figure 5

Figure S7, related to Figure 6

Supplementary figure legends

Table S1, related to Figures 1-5 (list of PCR primers and probes)

Table S2, related to Figure 6

Supplemental Experimental Procedures and References

Supplemental Data

The *In Vivo* Pattern of Binding of RAG1 and RAG2 to Antigen Receptor Loci

Yanhong Ji, Wolfgang Resch, Elizabeth Corbett, Arito Yamane, Rafael Casellas, and David G. Schatz

Supplementary Figure Legends

Figure S1. B and T cell development in D708A transgenic mice, Relates to Figures 1-4

(A and B) Flow cytometry analysis of bone marrow of young adult mice of the indicated genotypes with B220 (y-axis) and CD43 (x-axis) antibodies. In (A), note the large reduction of B220⁺/CD43⁻ cells in *Rag1*-deficient (R1^{-/-}) and D708A transgenic *Rag1*-deficient (D708A-R1^{-/-}) mice relative to WT, indicating a block in B cell development at the pro-B cell stage. In (B), note the large reduction in B220^{hi}/CD43⁻ mature B cells in *Rag1*-deficient B1-8i heavy chain knockin (R1^{-/-}-H) and D708A transgenic *Rag1*-deficient B1-8i heavy chain knockin (D708A-R1^{-/-}-H) mice relative to WT, indicating a block in B cell development at the pre-B cell stage. No IgM⁺ B cells could be detected in the spleens of D708A-R1^{-/-}-H mice (data not shown), indicating the absence of mature B cells in these mice.

(C and D) Flow cytometry analysis of thymocytes of young adult mice of the indicated genotypes with CD8 (y-axis) and CD4 (x-axis) antibodies. In (C), note the large reduction of CD4⁺CD8⁺ cells in *Rag1*-deficient (R1^{-/-}) and D708A transgenic *Rag1*-deficient (D708A-R1^{-/-}) mice relative to WT, indicating a block in T cell development at the pro-T (CD4⁺CD8⁻) cell stage. In (D), note the large reduction in CD4⁺CD8⁻ and CD4⁻CD8⁺ thymocytes in *Rag1*-deficient 2B4 Tcr β transgenic (R1^{-/-}- β) and D708A transgenic *Rag1*-deficient 2B4 Tcr β transgenic (D708A-R1^{-/-}- β) mice relative to WT, indicating a block in T cell development at the pre-T (CD4⁺/CD8⁺) cell stage.

Figure S2. RAG protein expression and Ig κ and Tcr α gene rearrangements in D708A transgenic mice, Relates to Figure 1

(A, B) Western blots of RAG1 and RAG2 expression in thymocytes (lanes 1-3) or CD19⁺ bone marrow B lineage cells (lanes 4-7) from mice of the genotypes indicated above the lanes. Ku80 was used as a loading control. WT, wild type.

(C) PCR assay for *Ig κ* recombination. Purified CD19⁺ bone marrow B-lineage cells from mice of the indicated genotypes were assayed for V-J κ recombination by PCR (33 cycles) using a reverse primer downstream of J κ 2 and a degenerate forward primer that recognizes a large fraction of V κ gene segments (Schlissel and Baltimore, 1989). Rearrangements are undetectable in D708A-R1^{-/-}-H mice, as is also the case in R1^{-/-}-H and *Rag2*-deficient B1-8i heavy chain knockin (R2^{-/-}-H) mice, indicating that the D708A RAG1 protein is inactive for V(D)J recombination. PCR for α -actin sequences was used as a control for DNA integrity.

(D) D708A *Rag1* does not support *Tcr α* locus recombination. DNA from thymocytes of the indicated genotypes was assayed by PCR for joining of TRAV12 family gene segments to five different J α gene segments, as indicated. PCR for α -actin sequences was used as a control for DNA integrity.

Figure S3. RAG binding to *Ig κ* in WT pre-B cells and lineage specificity of RAG binding, Relates to Figures 1-4

(A-C) Binding of RAG1 (A) or RAG2 (B), or levels of H3 acetylation (C) were assessed by ChIP

in WT B220⁺CD43⁻IgM⁻ FACS purified primary pre-B cells at the gene segments or regions indicated. The pattern of RAG binding resembles that observed in primary pre-B cells expressing D708A RAG1 and RAG2, with the exception of weak binding at J κ 1. This is likely the result of the extensive V-J κ recombination that has occurred in these cells. Recombination events involving J κ 1 disrupt the J κ 1 PCR reaction (the region amplified spans the J κ 1 RSS), rendering recombined alleles invisible to the assay. Consistent with this, amplification of the J κ 1 region was weak in the input DNA (data not shown). Furthermore, primary recombination events involving V κ and downstream J κ gene segments will move J κ 1 either onto an extrachromosomal circle (in the case of deletional recombination) or far from its original location and far from the Ig κ enhancer elements (in the case of inversional recombination). The weak RAG binding we observe at J κ 1 suggests that in either of these two cases, the RAG proteins do not bind efficiently to J κ 1. Weak signals for input and binding at Jh1 were also observed (not shown); presumably this reflects contaminating pro-B cells as well as detection of extrachromosomal circles created by recombination of Dh with downstream Jh gene segments. These considerations highlight the advantages of analyzing RAG binding in mice expressing D708A RAG1. Data are the average of 2 independent experiments and are presented as in Fig. 1.

(D, E) Binding of RAG1 (red bars) and RAG2 (blue bars) was assessed by ChIP in WT B220⁺CD43⁻IgM⁻ FACS purified primary pre-B cells (D) or in WT CD4⁺CD8⁺ FACS purified primary pre-T cells (E) at the gene segments or regions indicated. Data are the average of two independent experiments and are presented as in Fig. 1.

Figure S4. H3K4me3, RNA polymerase II, and H3 acetylation at the *Ig κ* locus in pre-B cells, Relates to Figure 1

(A-C) Levels of H3K4me3 (A), RNAP II (B) or H3 acetylation (H3-Ac) (C) were assessed by ChIP in primary CD19⁺ bone marrow B-lineage cells from Rag1^{-/-} B1-8i *Igh* knockin (R1-/-H), D708A transgene-positive Rag1^{-/-} B1-8i *Igh* knockin (D708A-R1-/-H), and Rag2^{-/-} B1-8i *Igh* knockin (R2-/-H) mice at the gene segments or regions indicated. Data are the average of 2 independent experiments and are presented as in Fig. 1.

Figure S5. Persistent RAG binding to *Igh* in pre-B cells and *Tcr β* in pre-T cells, Relates to Figures 2 and 4

(A, B) Binding of RAG1 (A) or RAG2 (B) were assessed by ChIP in primary CD19⁺ bone marrow B-lineage cells from Rag1^{-/-} B1-8i *Igh* knockin (R1-/-H), D708A transgene-positive Rag1^{-/-} B1-8i *Igh* knockin (D708A-R1-/-H), and Rag2^{-/-} B1-8i *Igh* knockin (R2-/-H) mice at the gene segments or regions indicated. Data are the average of 2 independent experiments and are presented as in Fig. 1. Note that DQ52 and Jh1-4 have been deleted on the B1-8i *Igh* knockin allele, so that only one *Igh* allele is assessed at these gene segments in these experiments.

(C, D) Binding of RAG1 (C) or RAG2 (D) were assessed by ChIP in primary thymocytes from Rag1^{-/-} 2B4 *Tcr β* transgenic (R1-/- β), D708A transgene-positive Rag1^{-/-} 2B4 *Tcr β* transgenic (D708A-R1-/- β), and Rag2^{-/-} 2B4 *Tcr β* transgenic (R2-/- β) mice at the gene segments or

regions indicated. Data are the average of three independent experiments and are presented as in Fig. 1. TRBJ2-5 and TRBJ2-7 were not analyzed because they are contained in the 2B4 *Tcr* β transgene.

Figure S6. RAG and recombination substrate expression in D345 cells infected with the pINV-12/23 or pINV-0 substrates, Relates to Figure 5

(A) Western blots of RAG1 and RAG2 expression before (0 hours) or 20 hours after induction with 3 μ M STI-571 in D345 cells infected with pINV-12/23 or pINV-0, as indicated above the lanes. A single membrane was sequentially incubated with RAG1 monoclonal antibody #14.1, RAG2 monoclonal antibody #8, and anti Ku80 antibodies. RAG1 and RAG2 were induced at least as well in pINV-0 infected cells as in pINV-12/23 infected cells.

(B) Expression of human CD4 (hCD4). Expression of pINV-12/23 and pINV-0 from the 5' LTR promoter was monitored by staining infected uninduced (blue lines) and induced (red lines) D345 cells with anti-human CD4-PE, which measures expression of the hCD4 gene contained downstream of the IRES in the substrates (see Fig. 5A, B). Staining intensity is plotted against relative cell number. 10,000 cells were analyzed for each condition. Average expression of hCD4 is at least as high in pINV-0 infected cells as in pINV-12/23 infected cells.

(C) H3K4me3 levels were assessed by ChIP in the D345 v-abl transformed cell line infected with pINV-12/23 (gray and red bars) or pINV-0 (white and blue bars) either prior to RAG induction (0hr) or after 20 hours of RAG induction (20hr) at the gene segments or regions indicated. Data are the average of two independent experiments and are presented as in Fig. 1. These data were derived from the same cells as used in the experiment of Fig. 5C, D.

Figure S7. The PHD domain of RAG2 contributes to binding to non-antigen receptor loci containing H3K4me3, Relates to Figure 6

(A, B) Binding of RAG2 (A) or levels of H3K4me3 were assessed in a R2^{-/-} v-abl pre-B cell line infected with a lentivirus expressing WT RAG2 (red bars) or W453A mutant RAG2 (blue bars) and a linked GFP gene. After lentiviral infection, cells were expanded and enriched for GFP expression by FACS (>80% GFP⁺ finally). Data were collected from cells 20 hours after treatment with STI-571 at the promoters of the genes indicated and are the average of two experiments derived from independent populations of infected cells. The *6430706D22Rik* (2Rik), *D030013116Rik* (6Rik), *Fahd1*, and *Mrsp5* genes were selected for analysis based on ChIP-seq experiments demonstrating that these genes are associated with high levels of H3K4me3 in the B cell lineage (not shown). Data for *Mrsp5* are shown on separate axes because of the strong RAG2 ChIP signal. No binding of RAG1 was detected by qPCR-ChIP at the *6430706D22Rik*, *D030013116Rik*, *Fahd1*, or *Mrsp5* loci in WT RAG2 or W453A RAG2 expressing cells (not shown).

(C) Western blot of lentiviral infected R2^{-/-} v-abl cells expressing WT RAG2 (lane 1) or W453A-mutant RAG2 (lane 2) proteins. As controls, protein from total thymocytes from Rag2^{-/-} 2B4 *Tcr* β transgenic (R2^{-/-} β) mice (lane 3) or D708A transgene-positive Rag1^{-/-} 2B4 *Tcr* β transgenic mice (which express WT RAG2) (lane 4). RAG2 monoclonal antibody #8 was used. The same blot was probed for Ku80 to assess protein loading.

Genotype of thymocytes	Antibody used for IP	Total sequencing reads passing quality filter	Uniquely aligned sequencing reads	Percentage aligned reads
Wild type	RAG2	15,836,506	7,566,851	48%
RAG2 ^{-/-}	RAG2	15,066,878	7,140,058	47%
D708A-R1 ^{-/-} β	RAG2	15,369,687	8,417,638	55%
D708A-R1 ^{-/-} β	H3K4me3	14,838,753	12,130,218	82%
Wild type	H3K4me3	11,921,334	7,612,684	64%

Table S2. Sequencing data for ChIP-sequencing analysis of total thymocytes.

SUPPLEMENTAL EXPERIMENTAL PROCEDURES

Generation of RAG1 D708A transgenic mice and mouse strains used

The D708A transgene was generated by altering the sequence of the *Rag1* open reading frame in the HG bacterial artificial chromosome (BAC) (Yu et al., 1999). A 2 kb fragment of *Rag1* in which the Asp708 codon GAT had been changed to GCG encoding alanine was inserted into the shuttle vector pSV1-RecA and introduced into the HG BAC by homologous recombination as described previously (Misulovin et al., 2001). The pattern of D708A BAC transgene expression in different founder lines was assessed by flow cytometry using GFP as a marker (data not shown), as described previously (Yu et al., 1999).

The following mouse strains were used: *Rag1*-deficient (Mombaerts et al., 1992), B1-8i *Igh* knockin (Sonoda et al., 1997), 2B4 *Tcr β* transgenic (Berg et al., 1989) or Bcl2 transgenic (Tg(BCL2)36Wehi (Strasser et al., 1991)) mice on a C57BL/6 background, and *Rag2*-deficient (Shinkai et al., 1992) mice on a mixed 129-C57BL/6 background.

Recombination substrates and cell lines

pINV-12/23 was generated from pMX-RSS-GFP/IRES-hCD4 (Liang et al., 2002) by replacement of the GFP cassette (EcoRI-NcoI fragment) with a fragment containing the mouse CD90 gene. pINV-0 was derived from pINV-12/23 by digestion with NotI-EcoRI, blunting with Klenow DNA polymerase, and recircularization to remove the 12RSS, and then digestion with NcoI-SnaBI, blunting with Klenow DNA polymerase, and recircularization to remove the 23RSS.

The WT pre-B cell line A70 was generously provided by B. Sleckman (Bredemeyer et al., 2006).

Flow cytometry

Developing lymphocytes were analyzed or purified by flow cytometry using a Becton-Dickinson FACS Caliber or FACS Aria. Cells were stained with one or more of the following antibodies from BD Biosciences: anti-mouse CD43-PE (#553271), anti-mouse B220-CyChrome (#553091), anti-mouse B220-CyChrome (#553091), anti-mouse IgM-APC (#550676), anti-mouse CD4-PE (#553653), anti-mouse CD8-PE-Cy5 (#553034), and anti-human CD4-PE (#555347).

RAG protein chromatin immunoprecipitation

A. Crosslinking and sonication of chromatin

Thirty million cells were resuspended in 9 ml RPMI/2% fetal bovine serum in a 15 ml conical tube and 0.25 ml of 37% formaldehyde (J. B. Baker #2106-10) were added and the tube rocked for 15 min at room temperature (RT). Glycine (American Bioanalytical #56-40-6) was added to a final concentration of 0.125 M using a 1.25 M stock solution (pH 7.4) to terminate crosslinking. Cells were pelleted (3K, 3 min, 4°C) and washed twice with 10 ml cold PBS. Wash solutions contained 1 mM PMSF and 1 µg/µl pepstatin A, which were included in all subsequent steps. After the second wash, cells were resuspended in 1 ml PBS and transferred to a 1.5 ml microfuge tube, pelleted (3K, 3 min, 4°C), and the supernatant removed. Unless used immediately, cell pellets were frozen on dry ice and stored at -80°C.

A cell pellet was resuspended in 600 µl RIPA buffer (10 mM Tris pH 7.4, 1 mM EDTA, 1% TritonX100, 0.1% sodium deoxycholate, 0.1% SDS) containing 0.8 M NaCl and incubated for 10 min on ice. Chromatin was sheared using a water bath sonicator (Diagenode) (4 x 5 min, high power) resulting in DNA of 300 to 500 bp. Samples were centrifuged (14K, 10 min, 4°C) and the supernatant transferred to a new microfuge tube. If not used immediately, 0.1 vol 50% glycerol was added and the sheared chromatin was stored at -80°C. Chromatin derived from 3-5 million cells was used for one ChIP experiment (one IP with a single antibody).

B. Pre-clearing of chromatin with Protein A beads

To create sufficient Protein A beads loaded with rabbit Ig to pre-clear the chromatin from 20 million cells, the following were mixed: 40 µl (bed volume) of Protein A agarose beads (Millipore #16-157), 40 µl normal rabbit serum (Invitrogen, #16120-099), and 40 µl PBS. The mixture was rocked for 15 min at RT, spun (3K, 1 min), the pellet washed twice with 1 ml RIPA (0.8 M NaCl), and the buffer removed.

The chromatin was then added to the rabbit Ig-loaded beads and rocked 1 hr at 4°C. Beads were spun down (3K, 2 min, 4°C) and the supernatant transferred to a new tube which contained a second batch of rabbit Ig-loaded beads, and rocked 1 hr at 4°C. Beads were spun out (3K, 2 min, 4°C) and the supernatant transferred to new tube. Any residual beads were spun out (14K, 10 min, 4°C) and the supernatant (precleared chromatin) carefully transferred to a new tube. The precleared chromatin was stored at -80°C in aliquots if not used immediately. An amount of chromatin equal to 10% of what would be used in a single IP was set aside for later use as the "input" sample.

C. Immunoprecipitation with anti-RAG antibody

Precleared chromatin was mixed with salmon sperm DNA (Stratagene, #201190-81) (final concentration 1.5 $\mu\text{g}/\mu\text{l}$), BSA (final concentration 0.5 $\mu\text{g}/\mu\text{l}$), and 5 μg anti-RAG1, anti-RAG2 or 5 μg normal rabbit IgG (Millipore #12-370) and rocked at 4°C overnight. The binding reaction was centrifuged to remove any particulate matter (14K, 10 min, 4°C) and the supernatant transferred to a new tube containing 5 μl (bed volume) protein A beads (preblocked with 2% BSA for 1 hr at RT). This mixture was rocked for 3 hr at 4°C, centrifuged (7K, 2 min, 4°C), and the beads washed three times (10 min, 4°C) with 1 ml RIPA (0.8 M NaCl) containing 1 mM DDT, 100 mM PMSF, then once (10 min, 4°C) with 1 ml RIPA (0.3 M NaCl) containing 1 mM DDT, 100 mM PMSF, then once (10 min, 4°C) with 1 ml RIPA containing 1 mM DDT, 100 mM PMSF, and finally once (10 min, 4°C) with 1 ml TE (10 mM Tris-HCl (pH 7.4), 1 mM EDTA). Beads were resuspended in 100 μl TE containing 50 μg Proteinase K and 0.25% SDS, and incubated at 60°C overnight. The "input" chromatin was treated identically. Proteinase K digests were extracted with 100 μl phenol/chloroform and after transferring the aqueous phase to a new tube, the organic phase was back extracted with 100 μl of water, and the aqueous phases were pooled. The aqueous material was extracted with 200 μl chloroform and after transferring the aqueous phase to a new tube, the organic phase was back extracted with 200 μl of water, and the aqueous phases were pooled. NaCl was added to a final concentration of 0.2 M and DNA precipitated with 20 μg glycogen and 1 ml ethanol. The DNA pellet was washed with 70% ethanol and resuspended in 50 μl water. The "input" sample was diluted 10-fold prior to PCR, so that input and IP samples would give \approx equal PCR signals if the IP had pulled down 1% of the locus under consideration.

PCR primers for quantitative PCR analysis

PCR primers for antigen receptor gene segments were designed to amplify a region adjacent to or spanning the RSS and were obtained from Invitrogen. Hydrolysis probes for qPCR were obtained from Biosearch Technologies. Table S1 provides primer and probe sequences as well as the distance from the relevant RSS in cases where the primers do not span the RSS. The $V_{\kappa}(\text{degen})$ and $V_{\kappa}220$ primers have been described previously (Curry et al., 2005). The primers and probes used to detect non-antigen receptor genes are also list in Table S1 and are located relative to the transcription start site of these genes as follows: α -actin, +3 to +61; β -actin, +77 to +144; β -globin, +147-+215; γ -actin, -571 to -494;

Eip4, +584 to +716; *Rars2*, +487 to +636. *Eip4* and *Rars2* were selected for analysis based on previously published data demonstrating that these genes have high levels of H3K4me3 near their transcription start sites in human T cells (Barski et al., 2007).

Tcr α rearrangements were detected by PCR (32 cycles) with primers for the TRAV12 gene segment family and various J α gene segments as described previously (Abarategui and Krangel, 2006).

ChIP analysis of mutant RAG proteins

For RAG1 expression, pMSCV2.2*EGFP (Fugmann et al., 2004) was altered by replacement of the EGFP gene with the gene for blastocystin resistance (Bsr), followed by insertion into the NotI and BglII sites of the full length murine RAG1 cDNA containing the D708A mutation or the D708A RAG1 cDNA containing mutations of three amino acids in the nonamer binding domain (NBD) (R391A, R393A, R402A). Retrovirus was prepared as described previously (Fugmann et al., 2004) and used to infect a R1^{-/-} v-abl pre-B cell line (11-3-4) containing a single copy integration of pINV-12/23. Individual Bsr-resistant clones were selected and induced with STI-571 for 20h and binding of RAG1 was assessed by ChIP. RAG1 protein levels were assessed using anti-RAG1 polyclonal antibodies.

A R2^{-/-} v-abl pre-B cell line (17-3-1) was infected with lentiviral vectors expressing WT RAG2 or RAG2 W453A kindly provided by S. Desiderio, R. Sen, and R. Subrahmanyam (Liu et al., 2007). Infected cells were subject to two rounds of sorting for GFP⁺ cells, resulting in a purity of greater than 80%. Cells were induced with STI-571 for 24 hours and RAG2 binding and H3K4me3 were assessed by ChIP. RAG2 protein levels were assessed using anti-RAG2 monoclonal antibody #8.

ChIP-Seq analysis

Immunoprecipitation of RAG2- or H3K4me3-bound DNA was performed as described above and following a published procedure (Barski et al., 2007) with the following changes: 2% fish skin gelatin (Sigma G7756) (Kolodziej et al., 2009) and 0.5 mg/ml heparin (Sigma H6279) were used in place of salmon sperm DNA as blocking agents and pull downs were performed using 25 μ l protein G magnetic beads (Invitrogen #100-03D) and a magnet instead of Protein A agarose beads. For the RAG2 antibody, three immunoprecipitations (each using chromatin from 30 x 10⁶ cells) were pooled to obtain sufficient DNA for sequencing.

The ChIP DNA ends were repaired using polynucleotide kinase and Klenow enzymes, followed by

treatment with Taq polymerase to generate a protruding 3' A base used for Illumina adaptor ligation. ChIP DNA was then amplified using adaptor primers for 17 cycles and fragments of approximately 200 bp (mononucleosome + adaptors) were isolated using an agarose gel. The purified DNA was used directly for cluster generation and sequencing analysis using the Solexa 1G Genome Analyzer following manufacturer protocols.

Sequence tags were mapped to the mouse genome (July 2007 assembly) using the Solexa Analysis Pipeline. To eliminate background noise signals, 200 bp tag "islands" for RAG2 and H3K4me3 were defined. An island was defined for each sample by first finding all summary windows that have more than one tag and then grouping consecutive windows above this threshold and allowing a distance of one window of empty signal. The output was then converted to browser extensible data (BED) files, which were uploaded into the UCSC genome browser (genome.ucsc.edu/) for visual analysis. Sequence tag parameters for the five ChIP-seq experiments performed are provided in Table S2.

SUPPLEMENTAL REFERENCES

Abarrategui, I., and Krangel, M.S. (2006). Regulation of T cell receptor-alpha gene recombination by transcription. *Nat. Immunol.* **7**, 1109-1115.

Barski, A., Cuddapah, S., Cui, K., Roh, T.Y., Schones, D.E., Wang, Z., Wei, G., Chepelev, I., and Zhao, K. (2007). High-resolution profiling of histone methylations in the human genome. *Cell* **129**, 823-837.

Berg, L.J., Pullen, A.M., Fazekas de St. Groth, B., Mathis, D., Benoist, C., and Davis, M.M. (1989). Antigen/MHC-specific T cells are preferentially exported from the thymus in the presence of their MHC ligand. *Cell* **58**, 1035-1046.

Bredemeyer, A.L., Sharma, G.G., Huang, C.Y., Helmink, B.A., Walker, L.M., Khor, K.C., Nuskey, B., Sullivan, K.E., Pandita, T.K., Bassing, C.H., *et al.* (2006). ATM stabilizes DNA double-strand-break complexes during V(D)J recombination. *Nature* **442**, 466-470.

Curry, J.D., Geier, J.K., and Schlissel, M.S. (2005). Single-strand recombination signal sequence nicks in vivo: Evidence for a capture model of synapsis. *Nat. Immunol.* **6**, 1272-1279.

Fugmann, S.D., Rush, J.S., and Schatz, D.G. (2004). Non-redundancy of cytidine deaminases in class switch recombination. *Eur. J. Immunol.* **34**, 844-849.

Kolodziej, K.E., Pourfarzad, F., de Boer, E., Krpic, S., Grosveld, F., and Strouboulis, J. (2009). Optimal use of tandem biotin and V5 tags in ChIP assays. *BMC Mol Biol* **10**, 6.

Liang, H.E., Hsu, L.Y., Cado, D., Cowell, L.G., Kelsoe, G., and Schlissel, M.S. (2002). The "dispensable" portion of RAG2 is necessary for efficient V-to-DJ rearrangement during B and T cell development. *Immunity* **17**, 639-651.

Liu, Y., Subrahmanyam, R., Chakraborty, T., Sen, R., and Desiderio, S. (2007). A plant homeodomain in

RAG-2 that binds Hypermethylated lysine 4 of histone H3 is necessary for efficient antigen-receptor-gene rearrangement. *Immunity* **27**, 561-571.

Misulovin, Z., Yang, X.W., Yu, W., Heintz, N., and Meffre, E. (2001). A rapid method for targeted modification and screening of recombinant bacterial artificial chromosome. *J Immunol Methods* **257**, 99-105.

Mombaerts, P., Iacomini, J., Johnson, R.S., Herrup, K., Tonegawa, S., and Papaioannou, V.E. (1992). RAG-1-deficient mice have no mature B and T lymphocytes. *Cell* **68**, 869-877.

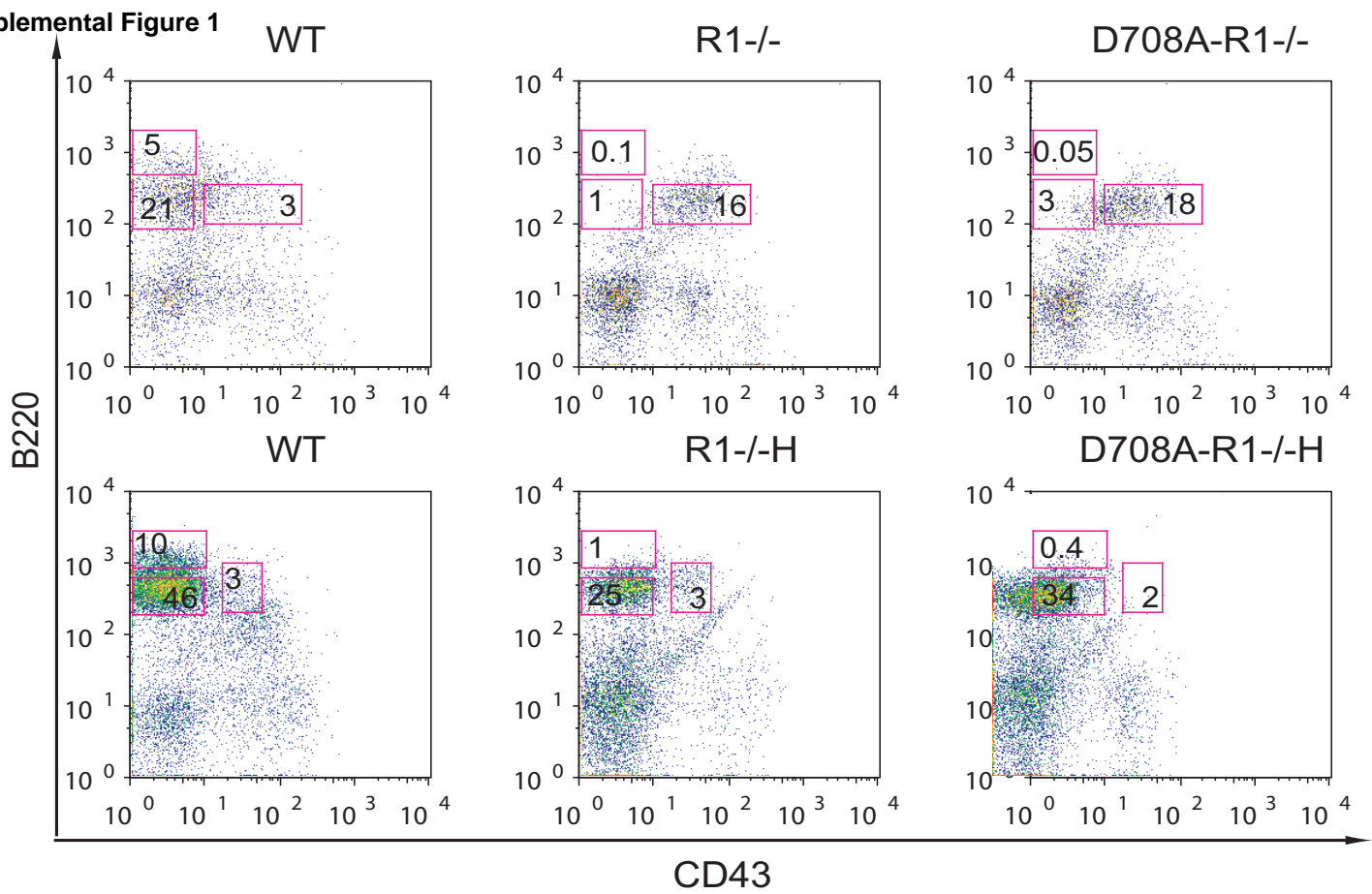
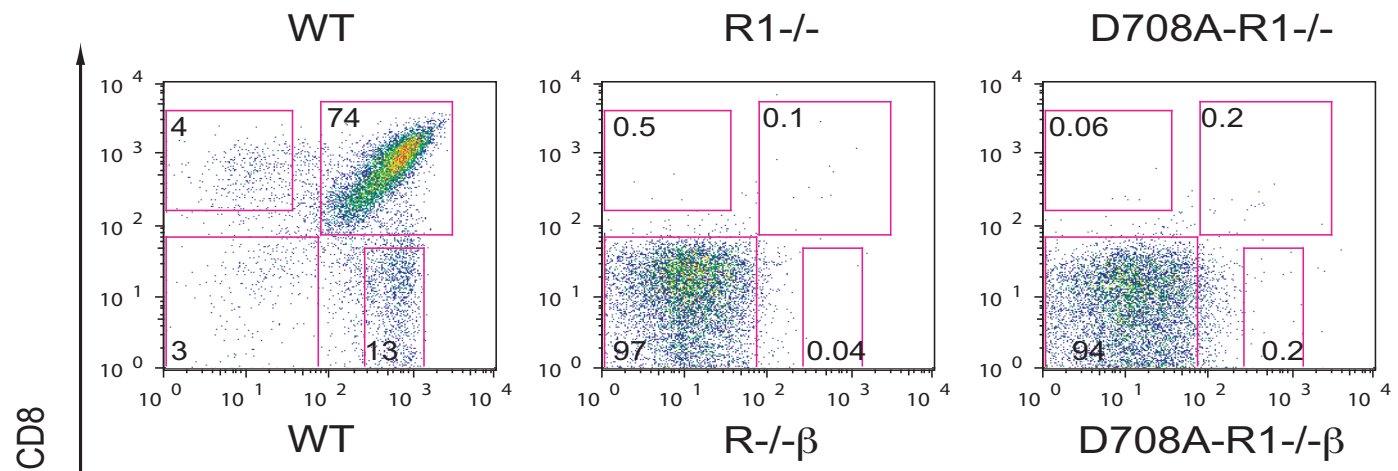
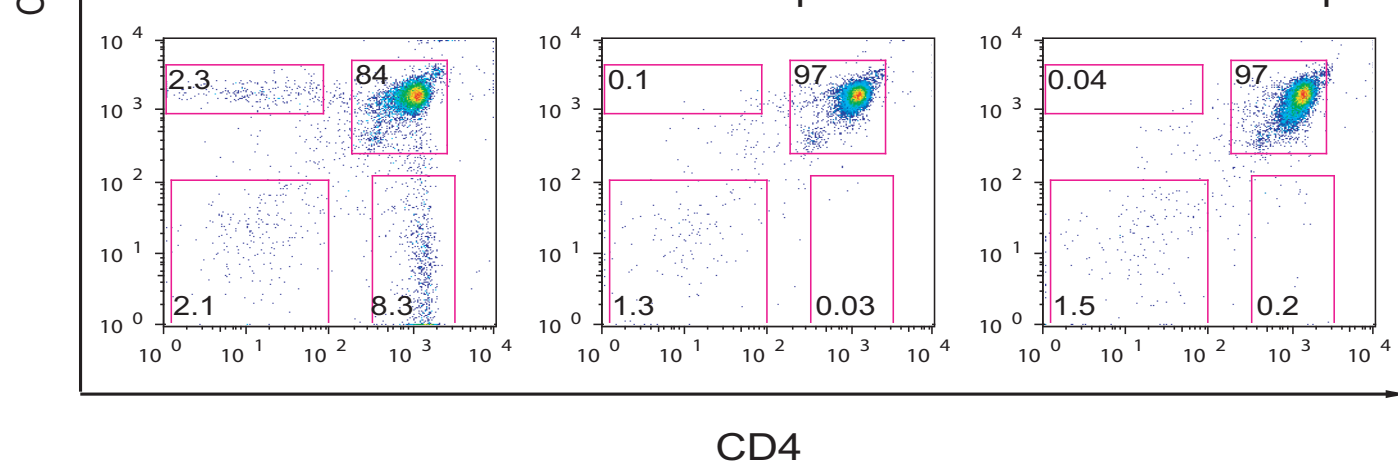
Schlissel, M.S., and Baltimore, D. (1989). Activation of immunoglobulin kappa gene rearrangement correlates with induction of germline kappa gene transcription. *Cell* **58**, 1001-1007.

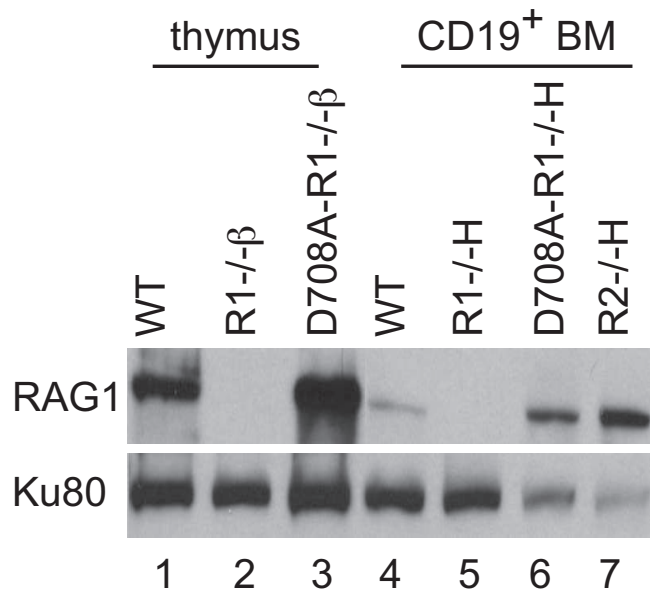
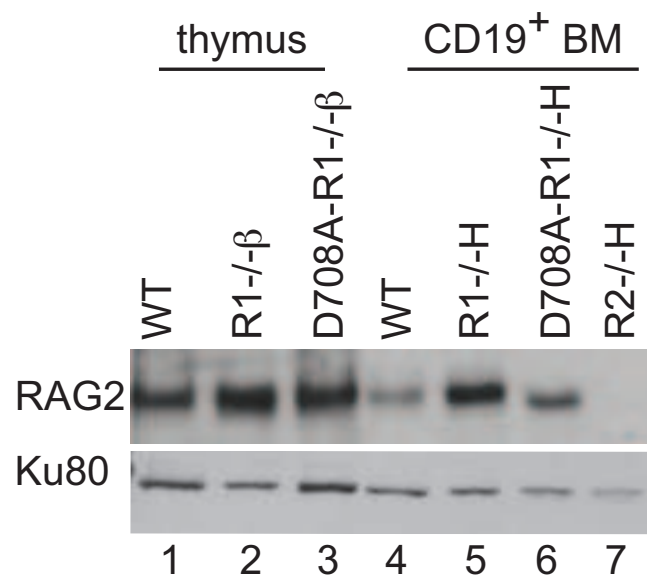
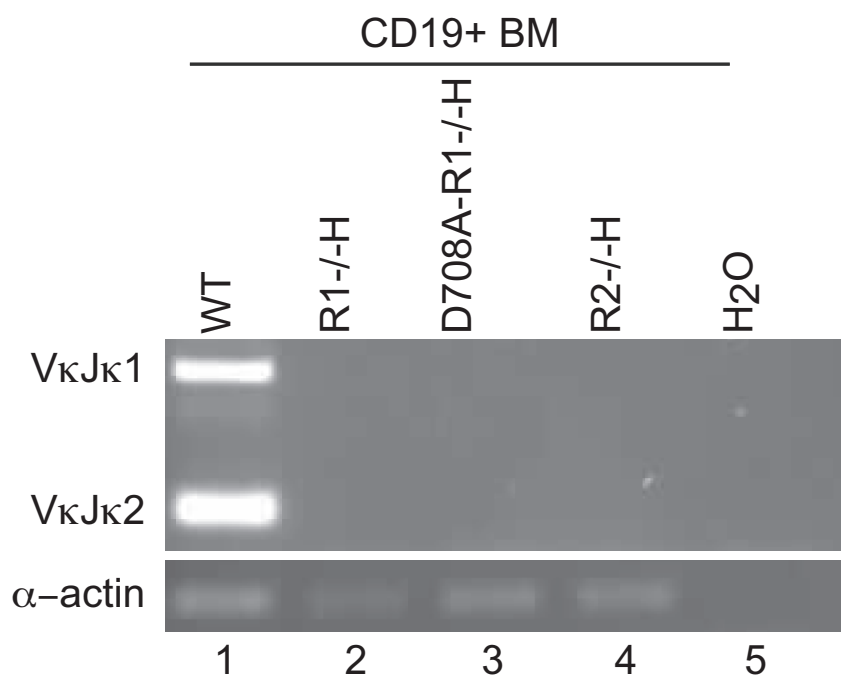
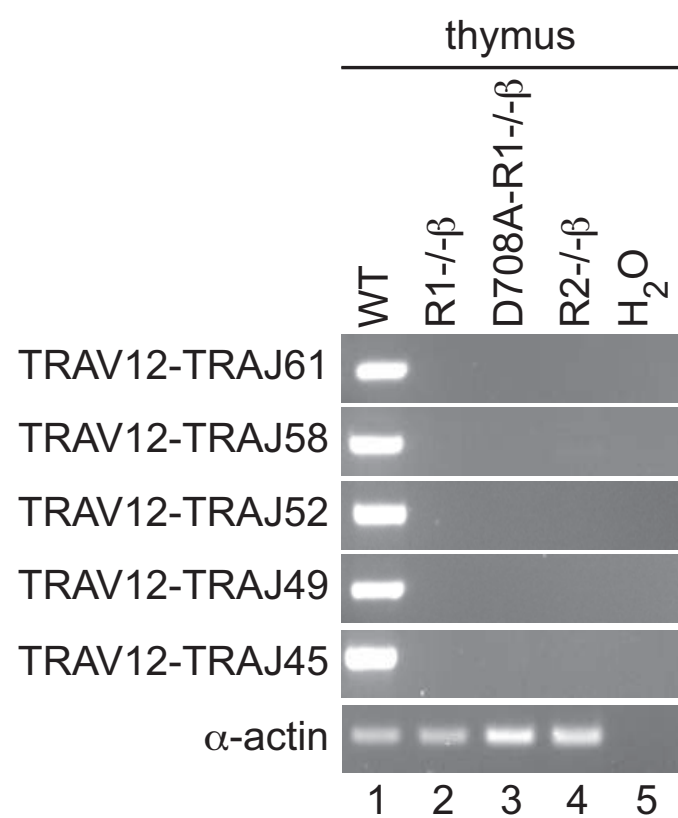
Shinkai, Y., Rathbun, G., Kong-Peng, L., Oltz, E.M., Stewart, V., Mendelsohn, M., Charron, J., Datta, M., Young, F., Stall, A.M., *et al.* (1992). RAG-2-deficient mice lack mature lymphocytes owing to inability to initiate V(D)J rearrangement. *Cell* **68**, 855-867.

Sonoda, E., Pewznerjung, Y., Schwers, S., Taki, S., Jung, S., Eilat, D., and Rajewsky, K. (1997). B cell development under the condition of allelic inclusion. *Immunity* **6**, 225-233.

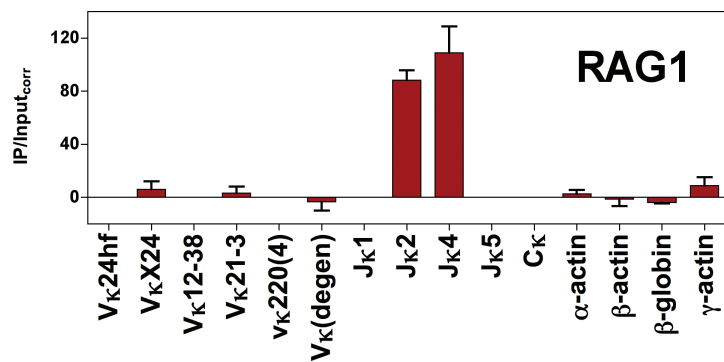
Strasser, A., Harris, A.W., and Cory, S. (1991). *bcl-2* transgene inhibits T cell death and perturbs thymic self-censorship. *Cell* **67**, 889-899.

Yu, W., Misulovin, Z., Suh, H., Hardy, R.R., Jankovic, M., Yannoutsos, N., and Nussenzweig, M.C. (1999). Coordinate regulation of RAG1 and RAG2 by cell type-specific DNA elements 5' of RAG2. *Science* **285**, 1080-1084.

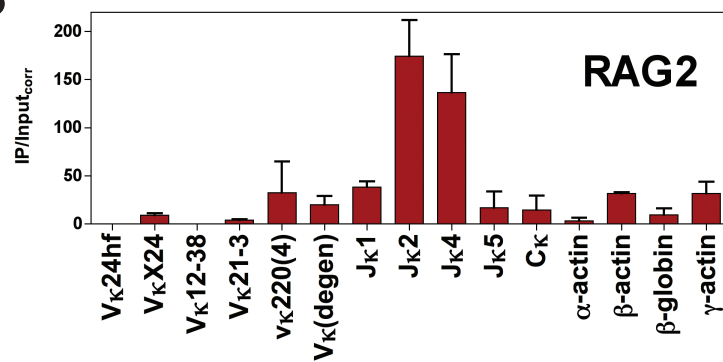
A Supplemental Figure 1**C****D**

A**B****C****D**

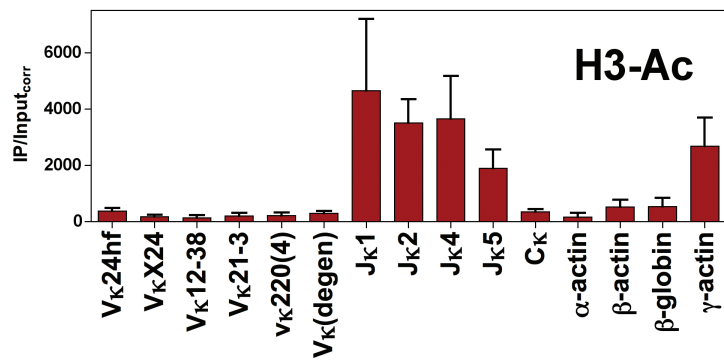
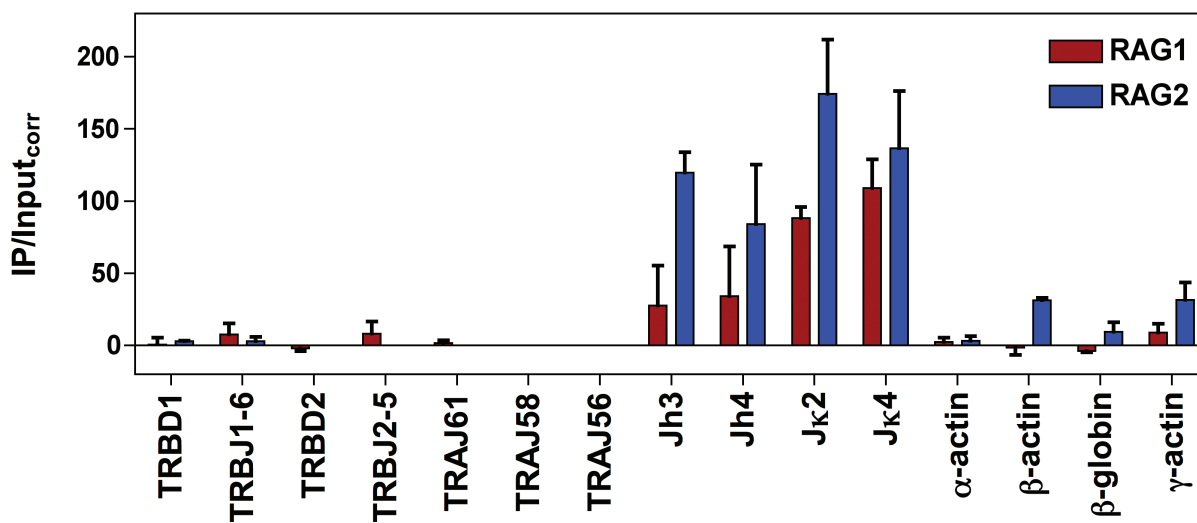
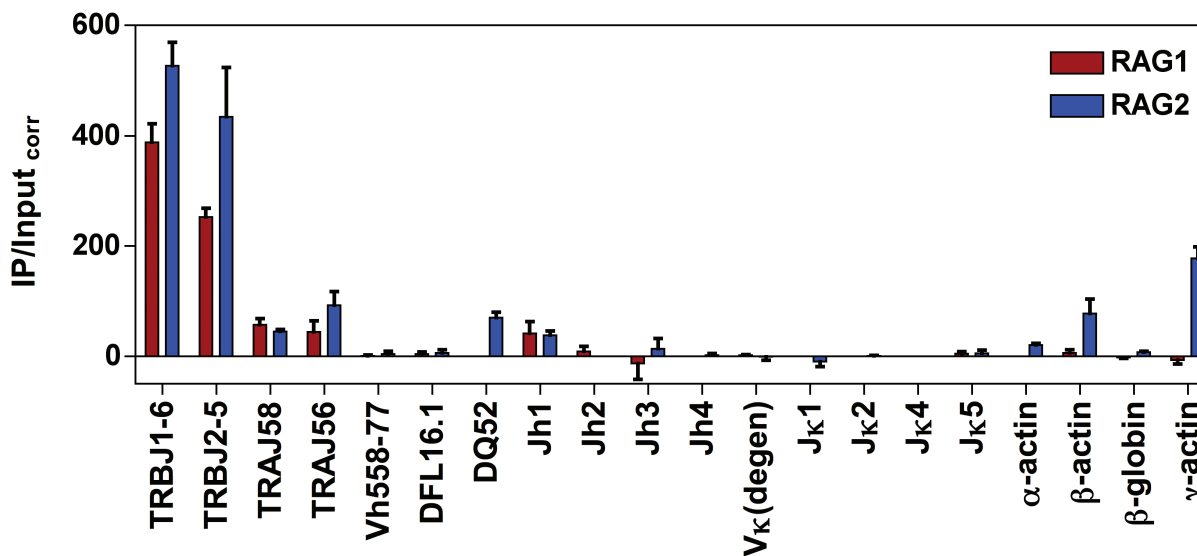
A



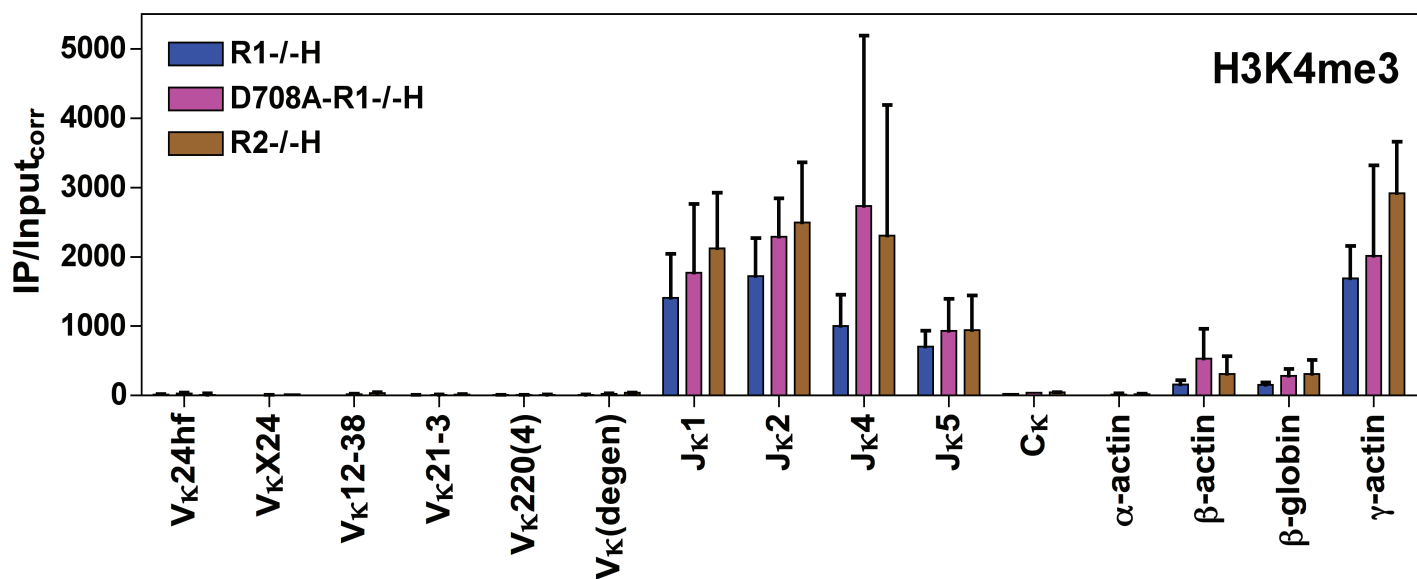
B



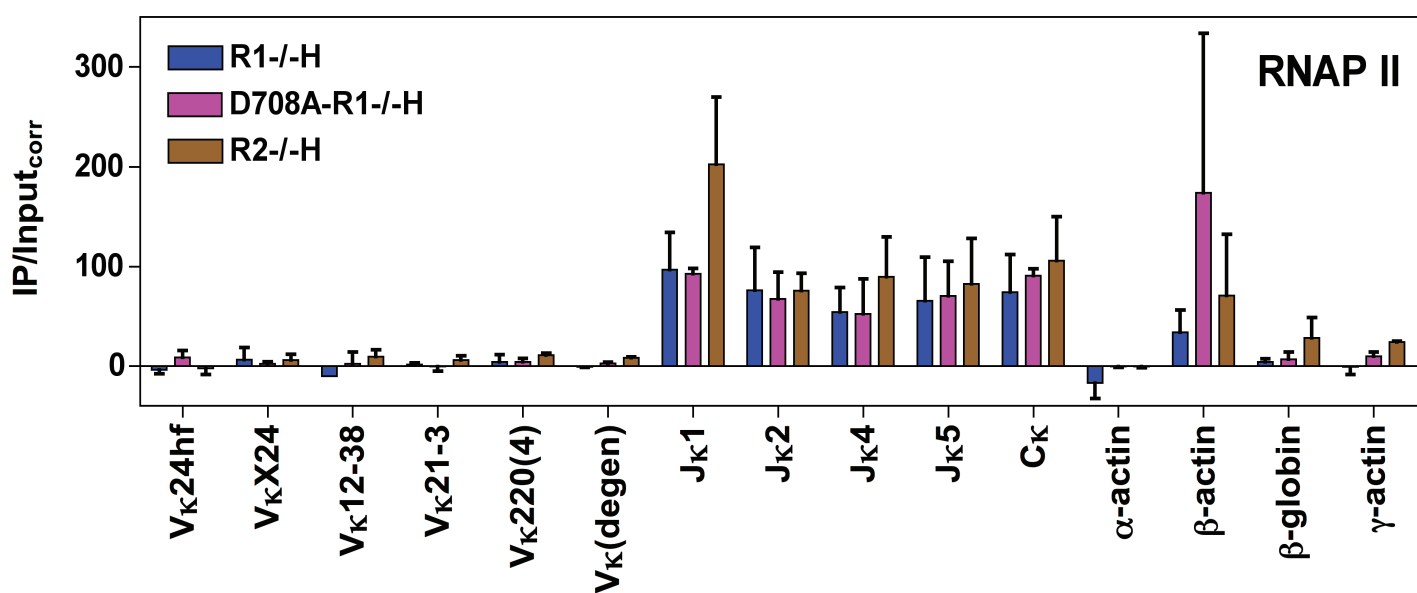
C

D B220⁺CD43⁻IgM⁻ pre-B cellsE CD4⁺CD8⁺ pre-T cells

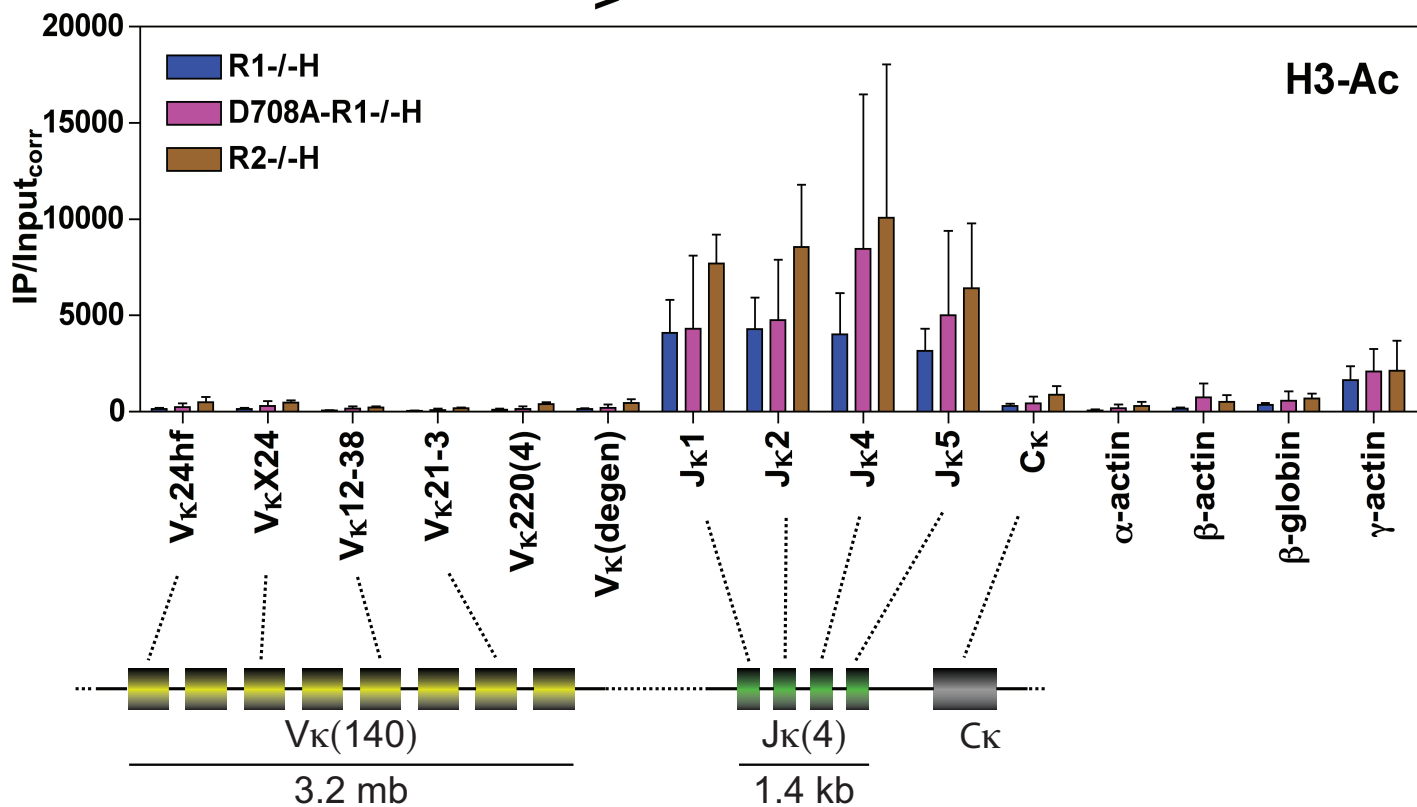
A

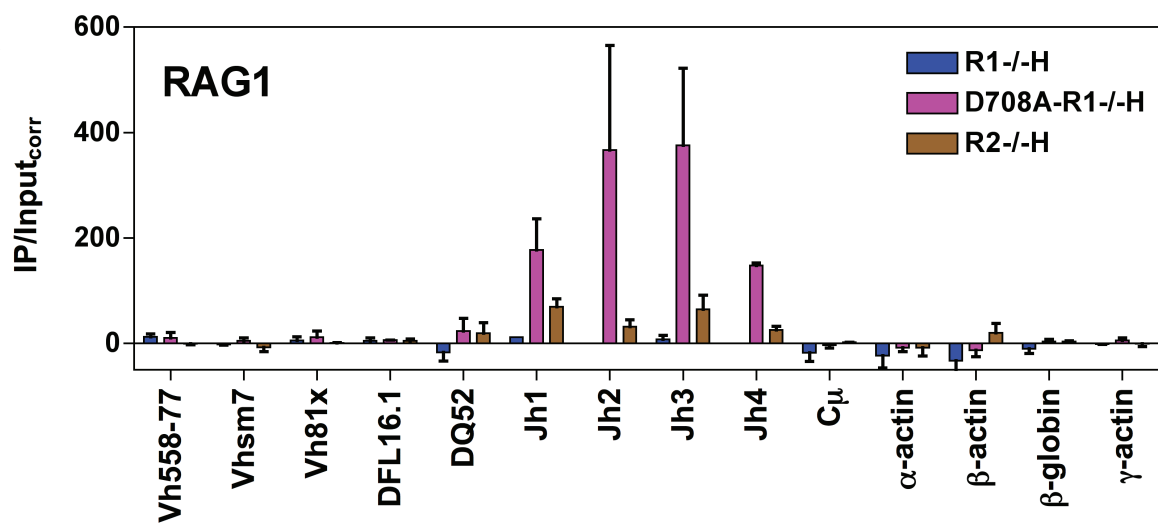
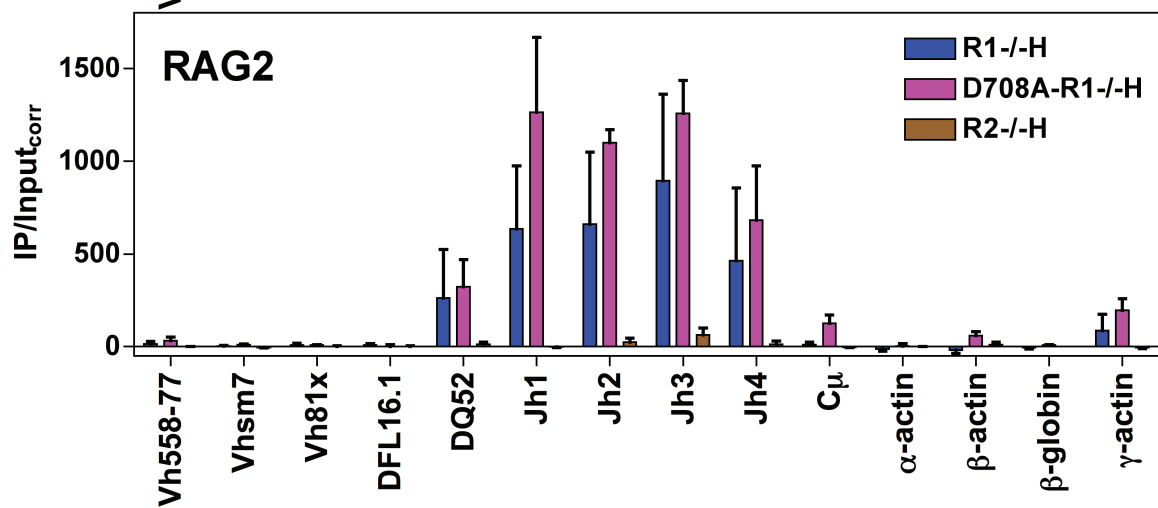
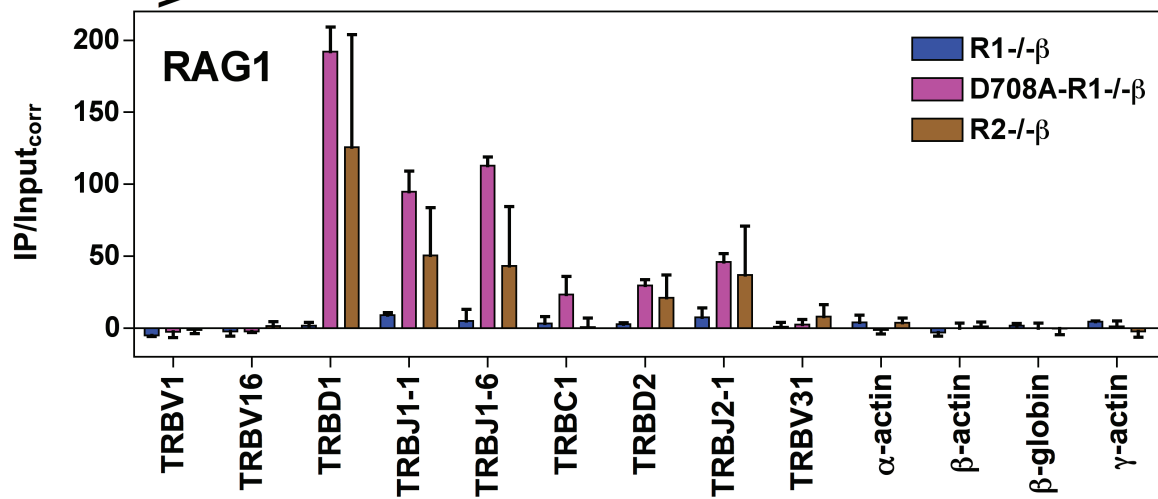
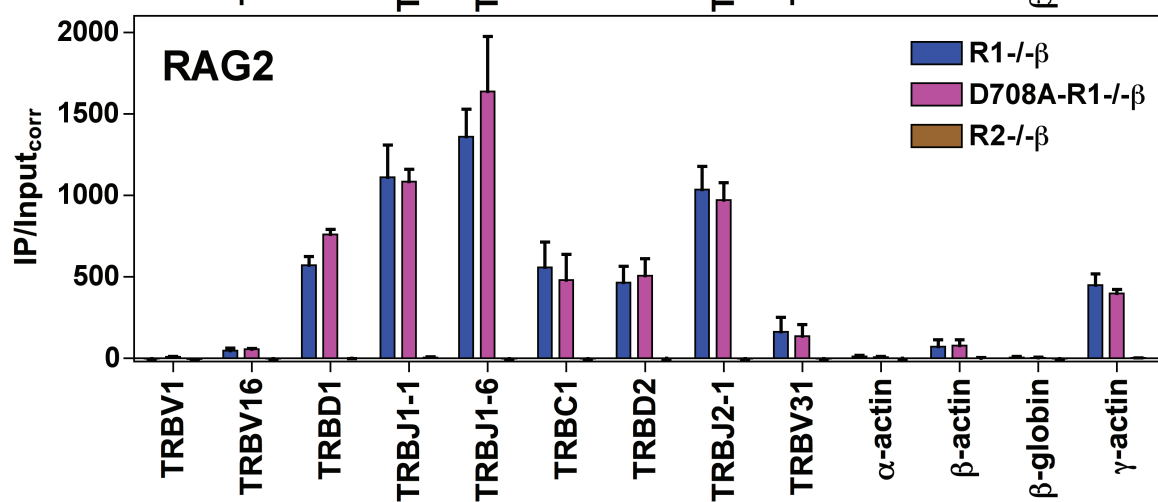


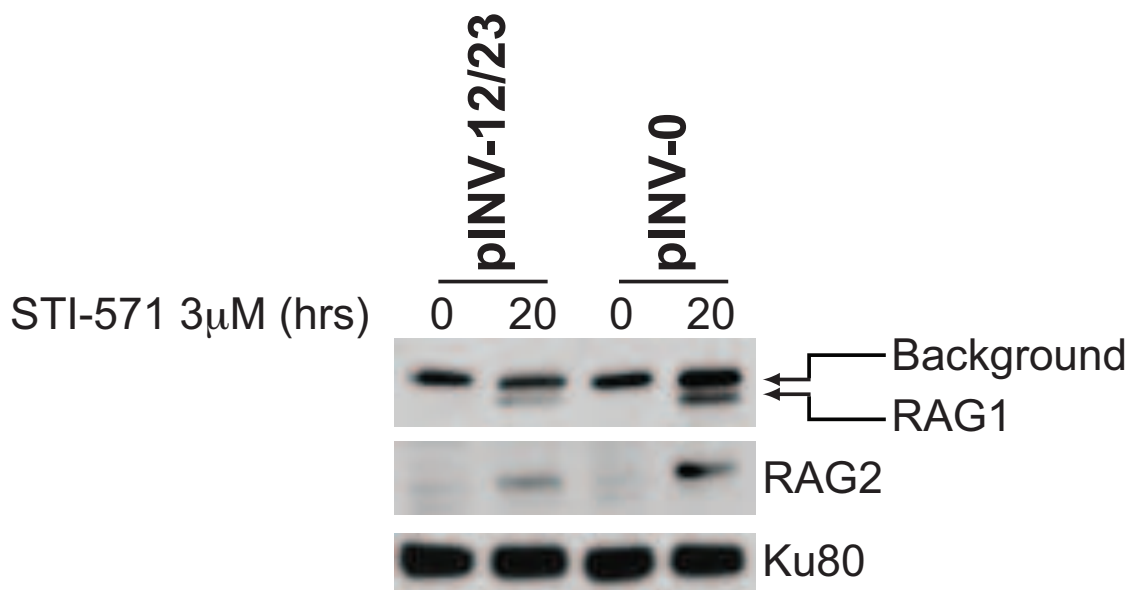
B



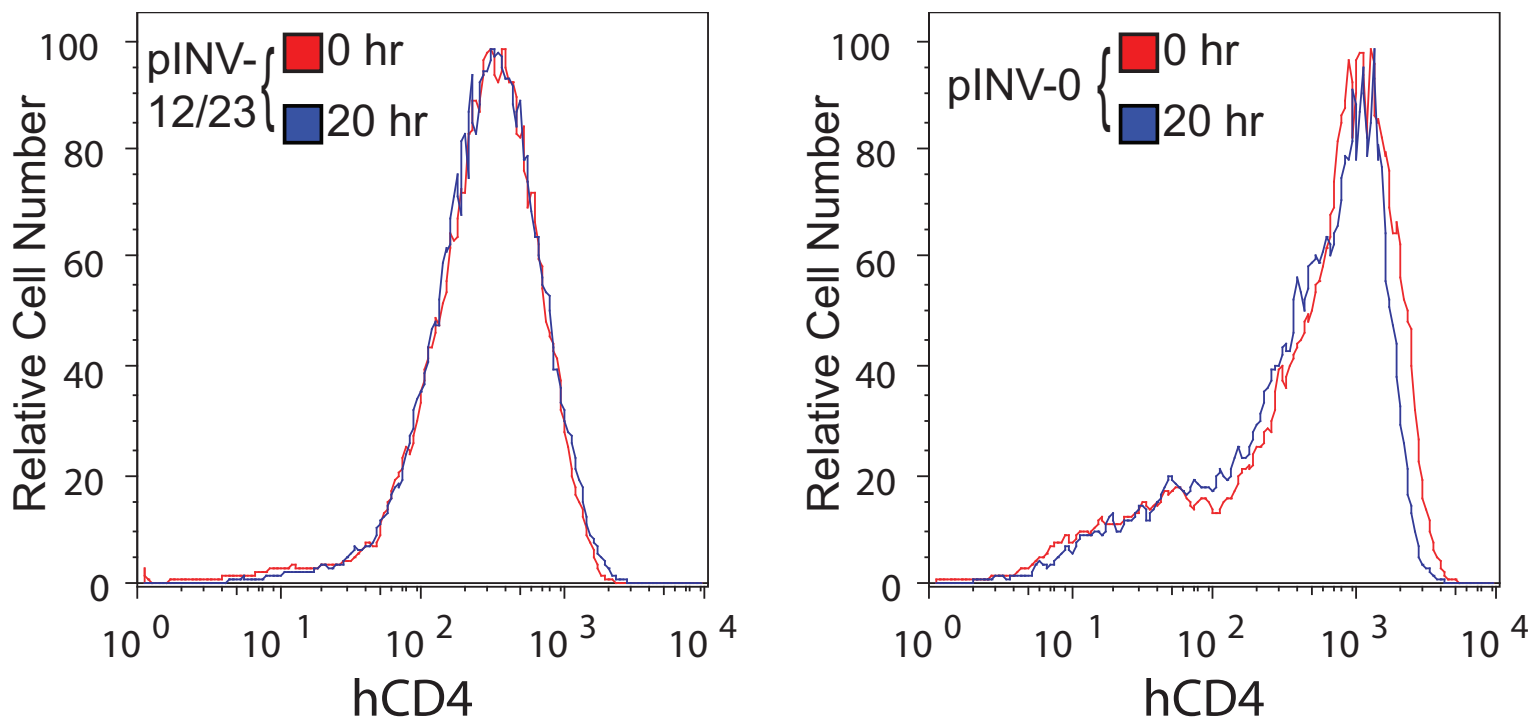
C



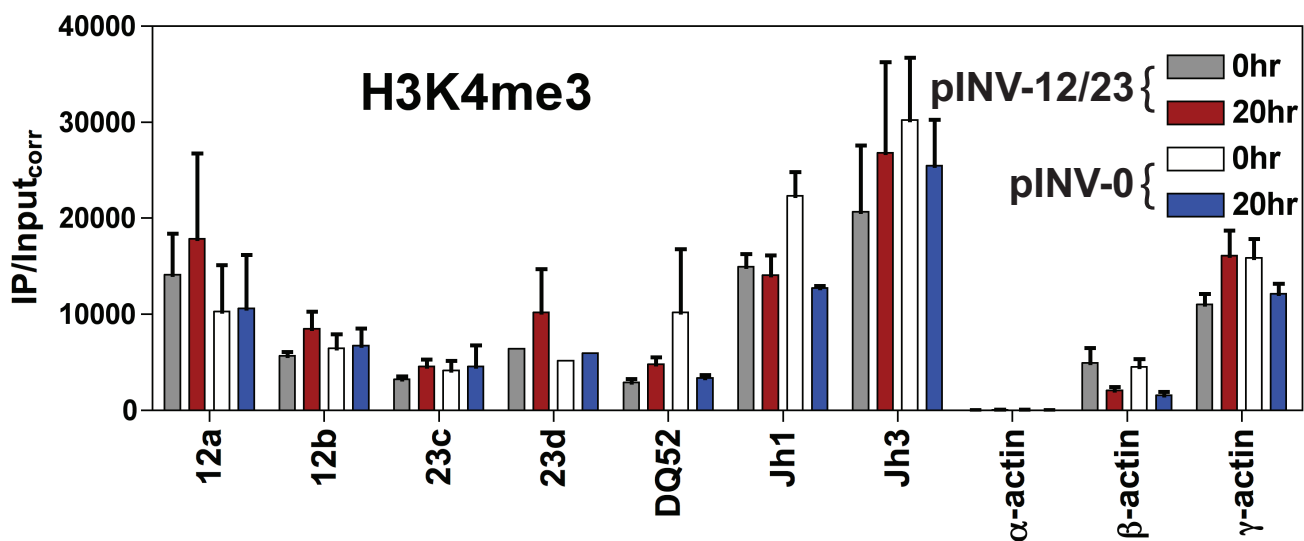
A**B****C****D**



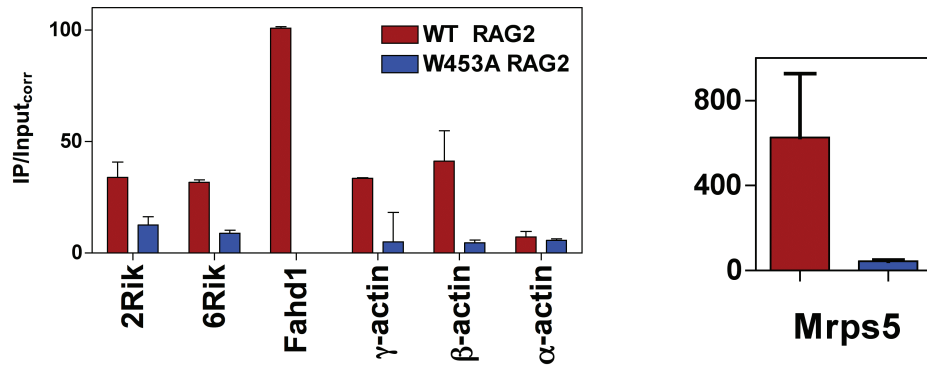
B



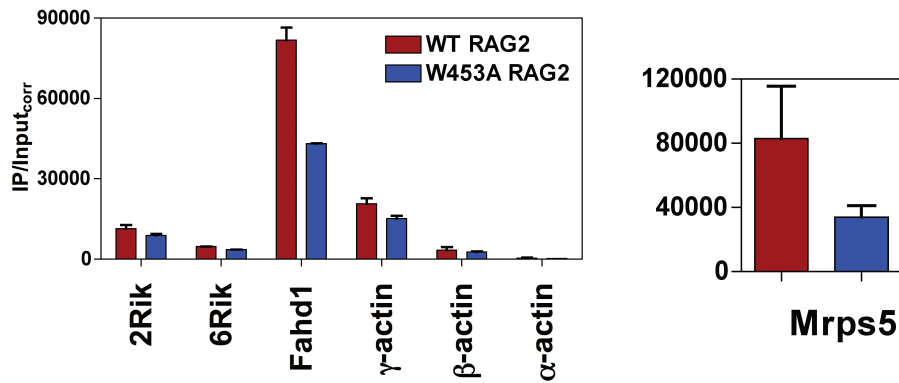
C



A RAG2 ChIP



B H3K4me3 ChIP



C

